Structure, Vol. 13, 579–590, April, 2005, ©2005 Elsevier Ltd All rights reserved. DOI 10.1016/j.str.2004.12.018

Structures of the N-Terminal and Middle Domains of *E. coli* Hsp90 and Conformation Changes upon ADP Binding

Qing Huai,[1,3] Huanchen Wang,[1] Yudong Liu,[1] Hwa-Young Kim,[1,4] David Toft,[2] and Hengming Ke[1,*]
[1]Department of Biochemistry and Biophysics and Lineberger Comprehensive Cancer Center
The University of North Carolina
Chapel Hill, North Carolina 27599
[2]Department of Biochemistry and Molecular Biology
Mayo Clinic and Foundation
200 First Street Southwest
Rochester, Minnesota 55905

Summary

Hsp90 is an abundant molecular chaperone involved in many biological systems. We report here the crystal structures of the unliganded and ADP bound fragments containing the N-terminal and middle domains of HtpG, an *E. coli* Hsp90. These domains are not connected through a flexible linker, as often portrayed in models, but are intimately associated with one another. The individual HtpG domains have similar folding to those of DNA gyrase B but assemble differently, suggesting somewhat different mechanisms for the ATPase superfamily. ADP binds to a subpocket of a large site that is jointly formed by the N-terminal and middle domains and induces conformational changes of the N-terminal domain. We speculate that this large pocket serves as a putative site for binding of client proteins/cochaperones. Modeling shows that ATP is not exposed to the molecular surface, thus implying that ATP activation of hsp90 chaperone activities is accomplished via conformational changes.

Introduction

Heat shock protein 90 (Hsp90) is the most abundant molecular chaperone, accounting for 1%–2% of the total protein in unstressed eukaryotic cells (Welch and Feramisco, 1982). In the early 1990s, several groups observed that Hsp90 was overexpressed at 2- to 10-fold higher levels in a wide variety of cancer cells and in virally transformed cells (Yufu et al., 1992; Ferrarini et al., 1992), suggesting a crucial role of Hsp90 for growth and/or survival of tumor cells. Hsp90 has been recognized as a unique target for the antitumor drug geldanamycin (Whitesell et al., 1998). The geldanamycin (GA) derivative, 17-allylamino-17-dementhoxy-geldanamycin (17AAG), inhibits all hallmark traits of malignant phenotypes and is potentially a general therapeutic for various cancers (Blagosklonny, 2002; Isaacs et al., 2003; Neckers, 2002; Goetz et al., 2003).

*Correspondence: hke@med.unc.edu
[3]Present address: Center for Homeostasis and Thrombosis Research, Beth Israel Deaconess Medical Center and Department of Medicine, Harvard Medical School, Boston, Massachusetts 02115.
[4]Present address: Department of Biochemistry, University of Nebraska-Lincoln, Lincoln, Nebraska 68588.

Hsp90 is involved in a diverse array of cellular processes such as signal transduction, cell cycle control, and transcriptional regulation (Pratt and Toft, 1997; 2003; Buchner, 1999; Caplan, 1999; Mayer and Bukau, 1999; Young et al., 2001; Picard, 2002; Prodromou and Pearl, 2003; Pratt et al., 2004). It is essential for the functions of a growing number of client proteins, of which over 100 are currently reported. These include steroid hormone receptors and the other transcription factors, protein kinases, calcineurin, nitric oxide synthase, tumor suppressors p53 and retinoblastoma, and telomerase (Smith and Toft, 1993; Mayer and Bukau, 1999; Pratt and Toft, 2003). To fulfill its function, Hsp90 acts as part of a multichaperone complex with a variety of cochaperones such as Hop/Sti1, FKBP52, cyclophilin 40, and p50/Cdc37 (Pratt and Toft, 1997; Hunter and Poon, 1997; Mayer and Bukau, 1999; Prodromou and Pearl, 2003; MacLean and Picard, 2003; Pratt et al., 2004). Hsp90 also incorporates heat shock protein 70 (Hsp70) and Hsp40 for activation of some client proteins.

Hsp90 is highly conserved in organisms from bacteria to mammals (Pratt, 1997; Csermely et al., 1998; Buchner, 1999; Pearl and Prodromou, 2000). The human genome contains four Hsp90 isoforms: cytosolic Hsp90α, Hsp90β, endoplasmic reticulum GRP94/gp96, and mitochondria TRAP1/Hsp75 (Pratt, 1997; Csermely et al., 1998; Buchner, 1999; Picard, 2002; Goetz et al., 2003). Human Hsp90 shares about 40% sequence identity and 55% similarity with the *E. coli* protein HtpG (high temperature protein G). On the basis of proteolytic data (Nemoto et al., 1997; Young et al., 1997), Hsp90 was shown to consist of an N-terminal geldanamycin/ATP domain, a middle domain, and a C-terminal dimerization domain. Except for TRAP1/Hsp75 and HtpG, other Hsp90s contain a highly charged region of about 55 amino acids linking the N-terminal and middle domains. An in vitro assay showed that Hsp90 possesses weak ATPase activity in the same order of magnitude as that of Hsp70 (Csermely and Kahn, 1991; Nadeau et al., 1992; 1993; Prodromou et al., 1997a; Panaretou et al., 1998; Scheibel et al., 1998). Binding and hydrolysis of ATP are essential for the in vivo molecular chaperone function of Hsp90 in yeast (Obermann et al., 1998; Panaretou et al., 1998; Siligardi et al., 2002).

Hsp90 is a member of the ATPase superfamily (GHKL) that includes DNA gyrase B/topoisomerase II (GyrB), DNA repair protein MutL, and histidine kinases CheA and EnvZ (Dutta and Inouye, 2000). Several crystal structures of Hsp90 are available: the N-terminal domain in complex with geldanamycin, ATP, or cochaperone Cdc37 (Stebbins et al., 1997; Prodromou et al., 1997a, 1997b; Obermann et al., 1998; Roe et al., 1999; Soldano et al., 2003; Jez et al., 2003; Roe et al., 2004; Immormino et al., 2004), the middle domain and its complex with cochaperone Aha1 (Meyer et al., 2003, 2004), and the C-terminal domain (Harris et al., 2004). On the basis of similarities in topological folding of the N-terminal and the middle domain, a "molecular clamp" model in which ATP drives association of the N-terminal

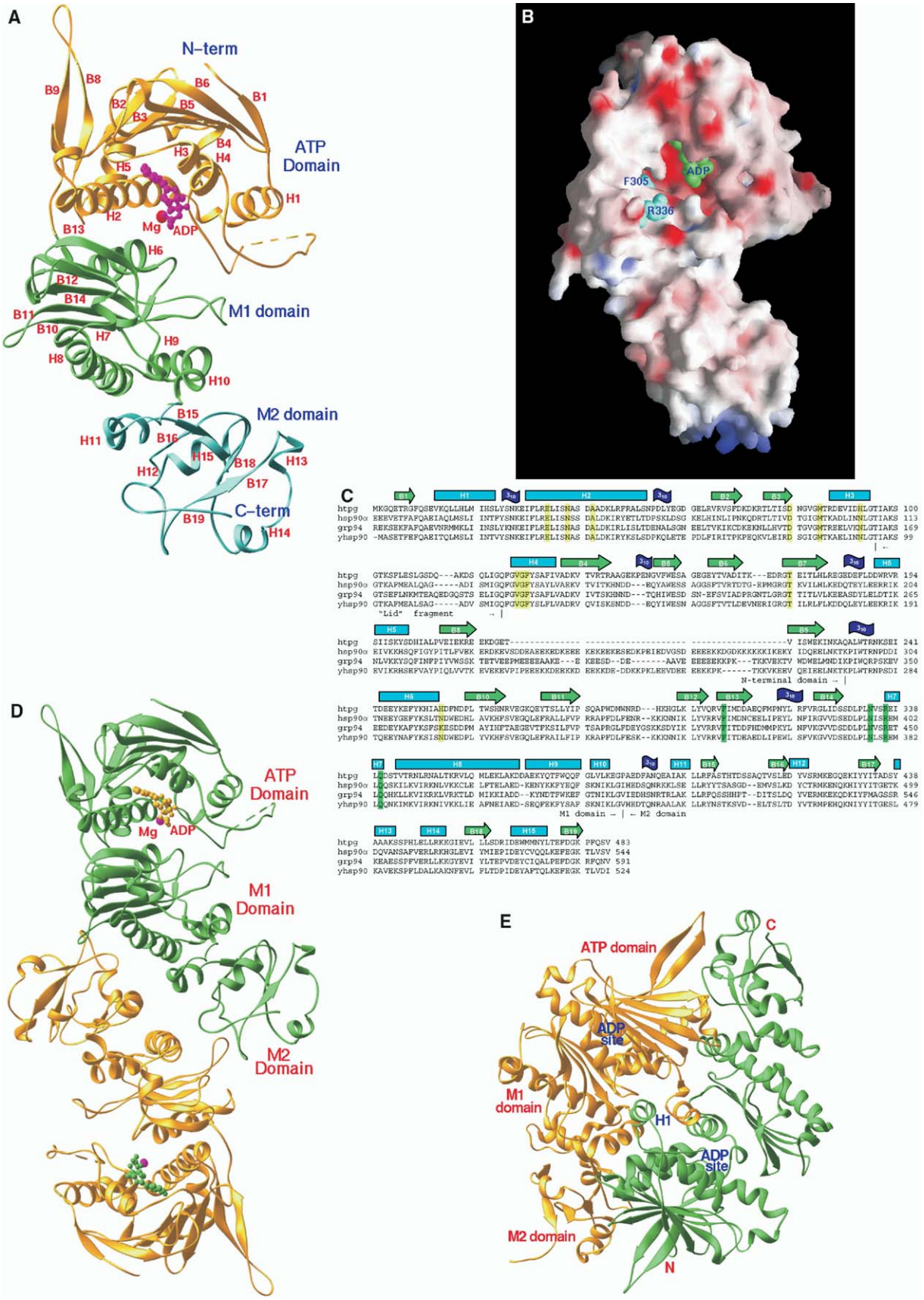
A
N–term
B9
B8
B6
B1
B2
B5
B3
ATP
Domain
B4
H3
H4
H5
H1
H2
Mg
ADP
B13
H6
B12
B14
M1 domain
B11
B10
H7
H9
H8
H10
B15
M2 domain
H11
B16
H15
B18
H13
H12
B17
C–term
B19
H14
B
F305
ADP
R336
C
htpg MKQETRGFQSEVKQLLHLM IHSLYSNKEIFLRELISNAS DAADKLRFPALSNPDLYEGD GELRVRVSFDKDKRTLTIGD NGVGMTREVIDHLGTIAKS 100
hsp90α EEEVETFAFQAEIAQLMSLI INTFYSNKEIFLRELISNSS DALDKIRYETLTDPSKLDSG KELKINLIPNKQDRTLTIVD TGIGMTKADLINNLGTIAKS 113
grp94 REKSEKFAFQAEVNRMMKLI INSLYKNKEIFLRELISNAS DALDKIRLISLTDENALSGN EELTVKIKCDKENNLLHVTD TGVGMTREELVKNLGTIAKS 169
yhsp90 -MASETFEFQAEITQLMSLI INTVYSNKEIFLRELISNAS DALDKIRYKSLSDPKQLETE PDLFIRITPKPEQKVLEIRD SGIGMTKAELINNLGTIAKS 99
htpg GTKSFLESLGSDQ---AKDS QLIGQFGVGFYSAFIVADKV TVRTRAAGEKPENGVFWESA GEGEYTVADITK---EDRGT EITLHLREGEDEFLDDWRVR 194
hsp90α GTKAFMEALQAG-----ADI SMIGQFGVGFYSAYLVAEKV TVITKHNDD---EQYAWESS AGGSFTVRTDTG-EPMGRGT KVILHLKEDQTEYLEERRIK 204
grp94 GTSEFLNKMTEAQEDGQSTS ELIGQFGVGFYSAFLVADKV IVTSKHNND---TQHIWESD SN-EFSVIADPRGNTLGRGT TITLVLKEEASDYLELDTIK 265
yhsp90 GTKAFMEALSAG-----ADV SMIGQFGVGFYSLFLVADRV QVISKSNDD---EQYIWESN AGGSFTVTLDEVNERIGRGT ILRLFLKDDQLEYLEEKRIK 191
"Lid" fragment
htpg SIISKYSDHIALPVEIEKRE EKDGET---------- ---------- ----------V ISWEKINKAQALWTRNKSEI 241
hsp90α EIVKKHSQFIGYPITLFVEK ERDKEVSDDEAEEKEDKEEE KEKEEKESEDKPEIEDVGSD EEEEKKDGDKKKKKKIKEKY IDQEELNKTKPIWTRNPDDI 304
grp94 NLVKKYSQFINFPIYVWSSK TETVEEPMEEEEAAKE---E KEESD--DE-------AAVE EEEEEKKPK---TKKVEKTV WDWELMNDIKPIWQRPSKEV 350
yhsp90 EVIKRHSEFVAYPIQLVVTK EVEKEVPIPEEEKKDEEKKD EEKKDE-DDKKPKLEEVDEE EEKKPK------TKKVKEEV QEIEELNKTKPLWTRNPSDI 284
N-terminal domain
htpg TDEEYKEFYKHIAHDFNDPL TWSHNRVEGKQEYTSLLYIP SQAPWDMWNRD---HKHGLK LYVQRVFIMDDAEQFMPNYL RFVRGLIDSEDLPLNVSREI 338
hsp90α TNEEYGEFYKSLTNDWEDHL AVKHFSVEGQLEFRALLFVP RRAPFDLFENR--KKKNNIK LYVRRVFIMDNCEELIPEYL NFIRGVVDSEDLPLNISREM 402
grp94 EEDEYKAFYKSFSKESDDPM AYIHFTAEGEVTFKSILFVP TSAPRGLFDEYGSKKSDYIK LYVRRVFITDDFHDMMPKYL NPVKGVVDSDDLPLNVSRET 450
yhsp90 TQEEYNAFYKSISNDWEDPL YVKHFSVEGQLEFRAILFIP KRAPFDLFESK--KKKNNIK LYVRRVFITDEAEDLIPEWL SPVKGVVDSEDLPLNLSREM 382
htpg LQDSTVTRNLRNALTKRVLQ MLEKLAKDDAEKYQTFWQQF GLVLKEGPAEDFANQEAIAK LLRFASTHTDSSAQTVSLED YVSRMKEGQEKIYYITADSY 438
hsp90α LQQSKILKVIRKNLVKKCLE LPTELAED-KENYKKFYEQF SKNIKLGIHEDSQNRKKLSE LLRYYTSASGD--EMVSLKD YCTRMKENQKHIYYITGETK 499
grp94 LQQHKLLKVIKKKLVRKTLD MIKKIADD--KYNDTFWKEF GTNIKLGVIEDHSNRTRLAK LLRFQSSHHPT--DITSLDQ YVERMKEKQDKIYFMAGSSR 546
yhsp90 LQQNKIMKVIRKNIVKKLIE APNEIAED-SEQFEKFYSAF SKNIKLGVHEDTQNRAALAK LLRYNSTKSVD--ELTSLTD YVTRMPEHQKNIYYITGESL 479
M1 domain → | ← M2 domain
htpg AAAKSSPHLELLRKKGIEVL LLSDRIDEWMMNYLTEFDGK PFQSV 483
hsp90α DQVANSAFVERLRKHGLEVI YMIEPIDEYCVQQLKEFEGK TLVSV 544
grp94 KEAESSPFVERLLKKGYEVI YLTEPVDEYCIQALPEFDGK RFQNV 591
yhsp90 KAVEKSPFLDALKAKNFEVL FLTDPIDEYAFTQLKEFEGK TLVDI 524
D
ATP
Domain
Mg
ADP
M1
Domain
M2
Domain
E
ATP domain
C
ADP
site
M1
domain
H1
ADP
site
M2 domain
N

domains into an active dimer has been proposed for GyrB, MutL, and Hsp90 (Wigley et al., 1991; Brino et al., 2000; Ban et al., 1999; Prodromou and Pearl, 2003). However, since no structure of an Hsp90 fragment bigger than a domain is available, it is unknown if the domain assembly of Hsp90 is the same as other ATPases and whether the GHKL ATPases act through a similar mechanism. We report here the crystal structures of a fragment 1–559 of *E. coli* Hsp90 (HtpG559) and its complex with ADP. The HtpG559 structures show that the N-terminal and middle domains assemble differently from those of GyrB and MutL, implying different mechanisms for the functions of these proteins. The structures also reveal several new features such as ADP-induced conformational changes and different dimerizations of HtpG.

Results and Discussion

Structure Architecture

In the structure of HtpG559-ADP-Mg (Figure 1), residues 1–108 and 119–483 are traceable, but residues 109–118 and 484–559 are not visible in the electron density maps and presumably exist in random conformations. The structure of the HtpG monomer (residues 1–483) can be divided into three subdomains: the N-terminal ATP binding domain (residues 1 to 231) and two middle domains of M1 (residues 232–386) and M2 (residues 387–483) (Figures 1A–1C). The N-terminal ATP binding domain in the HtpG559-ADP-Mg complex consists of a nine-strand β sheet (B1–B9) sided with five α helices (H1–H5). The M1 domain contains a central five-strand β sheet flanked with one and four helices on each side. The M2 domain also comprises a central five-strand β sheet flanked with three and two helices on each side. Our subdomain grouping is slightly different from an earlier proposal, in which the middle fragment of yeast Hsp90 was divided into three subregions of αβα, α coil, and αβα (Meyer et al., 2003). We integrated H9 and H10 of α coil region into the M1 domain and H11 of α coil region into the M2 domain for convenience of discussion.

The crystallographic asymmetric unit of the HtpG559-ADP-Mg complex contains two HtpG559 fragments that are associated into an apparent dimer in the crystals (Figure 1D). The superposition between two monomers of HtpG559 yields the root-mean-squared deviations of 1.0 Å for Cα atoms of the comparable residues in the whole chain, and 0.6, 0.6, and 1.0 Å, respectively, for the N-terminal, M1, and M2 domains, implying no significant variation of the domain orientations.

For the unliganded HtpG, SDS-PAGE of the crystals showed an apparent molecular weight similar to HtpG559 although the full-length HtpG (624 residues) was used in the crystallization, indicating proteolytic cleavage. The crystals of the unliganded HtpG contain a dimer of HtpG559 in the crystallographic asymmetric unit (Figure 1E) and have traceable regions of 1–100 and 120–489. The monomer of unliganded HtpG has similar folding and secondary structure elements to the HtpG559-ADP-Mg complex, except for the first 14 N-terminal residues (β strand B1) that are ordered in molecule A, but disordered in molecule B. The superposition between two monomers of the unliganded HtpG dimer yields rms deviations of 1.2 Å for Cα atoms of the comparable residues in the whole chain, and of 0.9, 0.5, and 0.6 Å for the N-terminal, M1, and M2 domains, respectively. The domain interface between the N-terminal and M1 domains is formed with several hydrogen bonds and van der Waals' interactions (see Table S1 in the Supplemental Data available with this article online). The domain orientation and the majority of the interdomain interactions are conserved between the unliganded and ADP bound structures of HtpG, but minor variations have been observed for the interdomain interactions. For example, the hydrogen bond between NH2 of Gln122 and ND1 of His255 in the unliganded HtpG has been replaced with the hydrogen bond between His255 and ADP in the ADP bound structure.

However, the dimerization scheme is completely different between the unliganded and ADP bound HtpG559 (Figures 1D and 1E). The dimer interface of the unliganded HtpG559 is formed with interactions between the N-terminal and middle domains, in addition to the contacts between helices H1. In contrast, the dimer interface in the HtpG559-ADP-Mg complex is formed with interactions between residues 238–477 of two middle domains. The total solvent-accessible surface area of the dimer changes from 44306 to 46813 $Å^2$ upon ADP binding. Associated with the different arrangement of the dimers, the pattern of hydrogen bonds and van der Waal's interactions are not comparable. The dimer of unliganded HtpG is tightly associated with 16 hydrogen bonds and massive hydrophobic interactions, in comparison with 6 hydrogen bonds and limited van der Waal's interactions in the ADP bound protein.

Structural Similarity of HtpG and Mammalian Hsp90

The overall molecular conformation of HtpG559 is similar to that of mammalian Hsp90s (Figure 2). A structural superposition between the N-terminal domains of HtpG559 and human Hsp90α yielded a root-mean-

Figure 1. HtpG Structure

(A) Ribbon presentation of the momomer of HtpG1-483 in the HtpG559-ADP-Mg complex (Carsons, 1991). ADP is shown as the pink sticks and Mg as the red ball. The N-terminal, M1, and M2 subdomains are presented in gold, green, and cyan colors. The missing residues are shown as the broken line. The correspondence of secondary structure element and sequence are shown in Figure 1C.

(B) Surface presentation of a monomer of HtpG1-483 (Nicholls et al., 1991). Red represents negative charges, blue is for positive charges. ADP (green balls) binds to the deep bottom of a putative site for binding of client proteins, which is jointly formed by residues of the N-terminal and middle domain. Residues Phe305 and Arg336, whose mutation suppressed yeast growth (Meyer et al., 2003), are shown in cyan balls.

(C) The alignment of secondary structures and amino acid sequences of HtpG, human Hsp90α, GRP94, and yeast Hsp90 (yhsp90). Residues highlighted with yellow are for binding of ADP. The residues highlighted with green in the middle domain are critical for yeast survival.

(D) Dimer of the HtpG-ADP-Mg complex.

(E) Dimer of the unliganded HtpG. Helices H1 make a mutual interaction in the dimer.

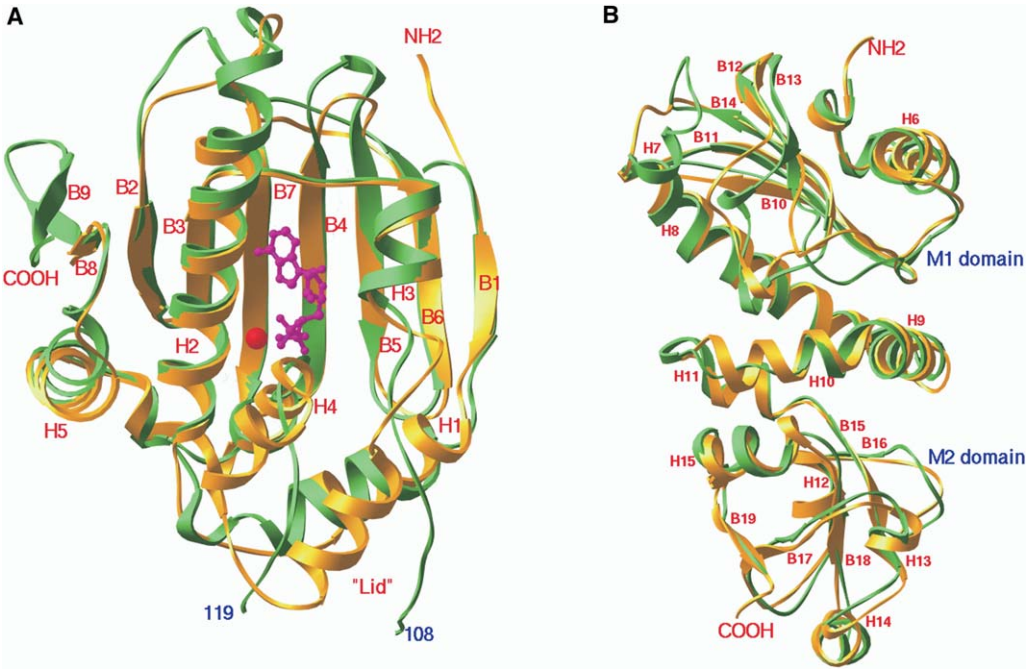

Figure 2. The Superposition between HtpG and Mammalian Hsp90s

(A) The N-terminal domains of human Hsp90α (golden) and HtpG (green). The lid fragment (between H3 and H4) shows dramatically differences in conformation. Residues 109–118 of HtpG are not traceable.

(B) The superposition between the middle domains of HtpG (green) and yeast Hsp90 (golden).

squared (rms) deviation of 1.2 Å for the Cα atoms of 167 comparable residues that were identified by the distance difference matrix analysis (Richards and Kundrot, 1988). Similar folding is also observed between the middle domains of HtpG and yeast Hsp90 (Meyer et al., 2003), as shown by the rms deviation of 1.4 Å for the Cα atoms of 233 comparable residues (244 residues total in the middle domains). Besides, the disordered C-terminal residues 484–559 in the HtpG559 structures is coincident with the structure of the middle fragment (residues 273–560) of yeast Hsp90, in which residues 526–560 (485–521 of the HtpG equivalents) are disordered in the crystal (Meyer et al., 2003). However, the recent structure of the C-terminal domain of HtpG (residues 511–624) showed an ordered conformation of residues 511–559 (Harris et al., 2004). This disagreement likely indicates the conformational flexibility of the region and its dependence on environment.

However, different conformations between HtpG and mammalian Hsp90 are observed for the "lid" fragment that is involved in ATP binding (Prodromou and Pearl, 2003). This loop of HtpG (residues 96–124) contains no secondary structure elements and the majority of the residues are disordered in both the unliganded and ADP bound crystals. In contrast, the "lid" fragments of yeast and human Hsp90 as well as GRP94 are ordered and contain two helices (Prodromou et al., 1997a; Stebbins et al., 1997; Soldano et al., 2003).

A finding of our structural study is that the charged linker in the mammalian Hsp90s may physically belong to the N-terminal domain. The HtpG559 structure shows an extra β strand B9 (residues 221–226) in the N-terminal domain, which corresponds to residues 284–290 of human Hsp90α after the charged linker (Figures 1A and 1C). Although HtpG does not contain the charged loop (Figure 1C), the positions of two β strands B8 and B9 predict that the charged fragments in mammalian Hsp90s orient to a surface of the N-terminal domain (Figure 1A). This assumption is different from the traditional view that the charged linker acts as a flexible tether to connect the N-terminal and middle domains (Prodromou and Pearl, 2003). Our argument is supported by the N-terminal crystal structure of human endoplasmic reticulum GRP94 (Soldano et al., 2003), in which the corresponding β strand (residues 330–335) after the charged linker occupies the B9 position. Thus, this region is likely to serve as a highly charged surface for interactions with proteins, and not as a linker between domains, as suggested earlier (Chadli et al., 2000).

ADP Binding to a Subpocket of a Large Site

The ($2F_o - F_c$) map shows that ADP and a magnesium ion bind to a subpocket of a big site formed by residues of the N-terminal and M1 domains (Figures 1A, 1B, 3A, and Figure S1). ADP is partially buried in the bottom of the subpocket made up of the residues from helices H2, H3, H4, and strands B3, B4, and B7 (Figures 3A and 3B). The solvent-accessible surface area of ADP is about 25% of its total surface area. The oxygen atoms of the α- and β-phosphates form hydrogen bonds with OD1 and ND2 of Asn38, ND1 of His255, and with backbone nitrogen of Phe127. The adenine ring of ADP takes an anti-configuration, and its N1 and N6 atoms form hydrogen bonds with OD2 of Asp80 and OG1 of Thr174, respectively. In addition, ADP makes hydrophobic and polar interactions with residues Glu34, Ala42,

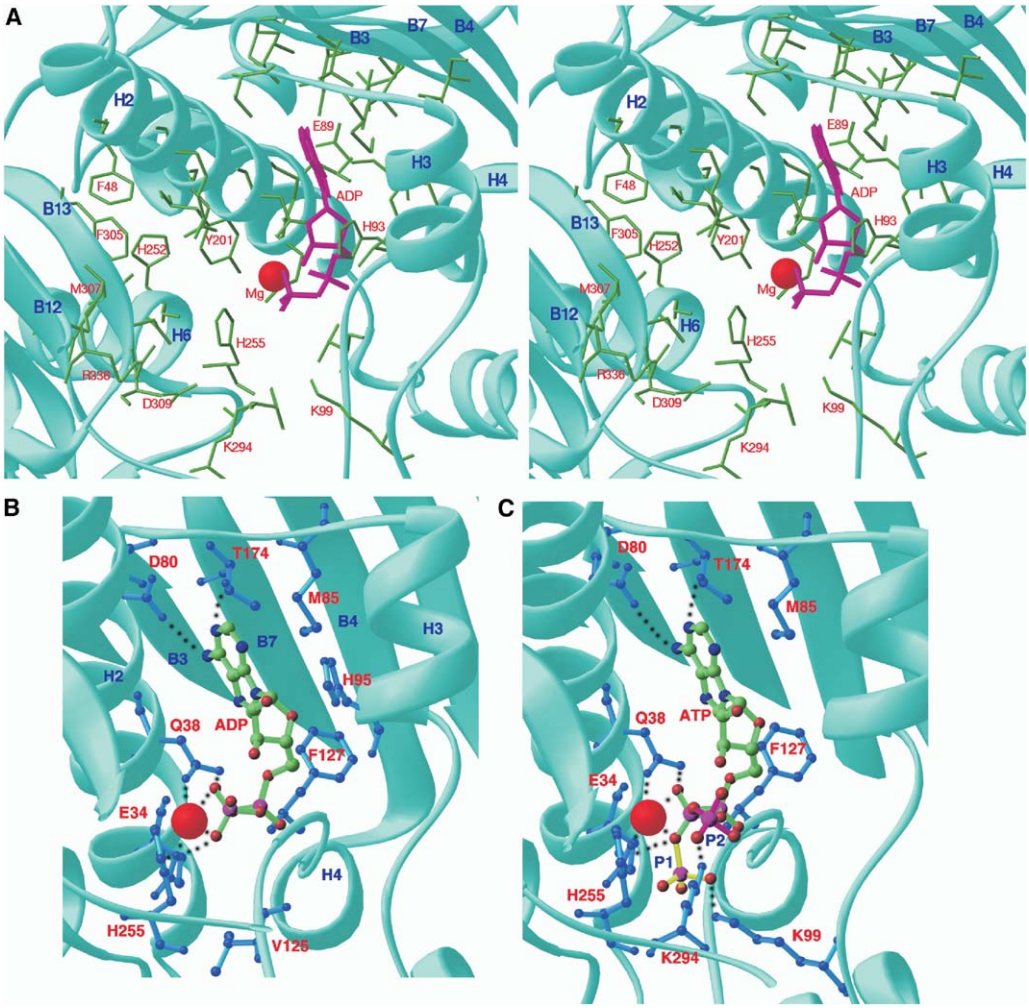

Figure 3. ADP Binding to HtpG

(A) Stereoview of ADP binding (pink sticks) to a subpocket of a putative pocket for binding of a client protein/cochaperone. The pocket is formed by residues from the N-terminal (H2, H3, H4, B3, B4, and B7) and middle (H6, H7, B12, and B13) domains.

(B) The detailed interactions between ADP and HtpG. The HtpG residues are shown as blue stick-balls. The magnesium ion is shown as a big red ball. The dotted lines represent hydrogen bonds or coordinations with magnesium.

(C) Model of ATP binding to HtpG. There are at least two ways to model the γ-phosphate of ATP. The first orientation of the γ-phosphate of ATP (marked as P1 and yellow bonds) is taken from the conformation of ADPNP in GyrB (Brino et al., 2000) and potentially interacts with Lys99 of HtpG. Alternatively, the γ-phosphate of ATP may orient toward the middle domain, as marked as P2, and its bonds are colored with pink. This orientation may be stabilized by a hydrogen bond with Lys294 from the middle domain.

Met85, His93, Val125, Gly126, and Phe127. The magnesium ion is coordinated with the oxygen atoms of α- and β-phosphates of ADP, OD1 of Asn38, and OE1 of Glu34. Sequence alignment shows that 9 out of 11 ADP-Mg^{2+} binding residues are identical and the remaining 2 residues (His93 and His255) are conserved among the Hsp90 family (Figure 1C). This observation implies that HtpG is an ATPase, as reported early (Owen et al., 2002). We measured the ATP activity of HtpG with the method of enzyme-coupled assay on the NADH hydrolysis (Ali et al., 1993) and observed that the purified protein of full-length HtpG has a typical specific activity of 1.5 μM ATP/min/μM HtpG at room temperature. This number is comparable with the specific activity of 1.05 μM ATP/min/μM yeast Hsp90 at 37°C (Richter et al., 2002).

Our study of the HtpG N+middle domain construct reveals two novel features that have not been seen in structures of isolated Hsp90 domains. First, an oxygen atom of β-phosphate of ADP forms a hydrogen bond with ND1 of His255 of the M1 domain of HtpG, suggesting involvement of the middle domain in the ATP hydrolysis. This observation is consistent with biochemical studies showing that residues 1–450 are required for the ATP hydrolysis (Weikl et al., 2000). Second, the ADP binding site of the N domain (Prodromou et al., 1997a; Obermann et al., 1998; Immormino et al., 2004) is in fact a subpocket of a bigger site composed of structural elements from both the N and middle domains (Figures 1B and 3A). The residues of the N-terminal domain (H2, H3, H4, B3, B4, and B7) form one wall of the site while the residues of the M1 domain (H6, H7, B12, and B13) constitute another wall (Figure 3A). ADP binds to the deep bottom on the N-terminal side and occupies

about 40% volume of the site (Figures 1B and 3A). The remaining portion of the site is open to the molecular surface and contains a mixture of hydrophobic and charged residues. In this pocket, residues Phe48, Leu51, Val304, Phe305, and Ile306 form a hydrophobic patch that is neighboring the charged residues of Asp41, Asp44, Lys45, Lys294, Lys298, Asp308, and Arg336. These residues are absolutely conserved in Hsp90s from bacteria to mammals except for Phe48 and Lys294 (Figure 1C), implying their important roles in the biological functions. The hydrophobic patch in the neighborhood of the ADP binding site makes this pocket a strong candidate as a binding site for a client protein or a cochaperone. This argument is supported by mutagenesis data in which the F349A and R380A mutations of yeast Hsp90 (Phe305 and Arg336 of HtpG) dramatically suppress yeast growth and v-Src activation (Meyer et al., 2003).

Our structural information on ADP binding can aid in understanding the mutagenesis data. The observation that mutations of E33A and D79N of yeast Hsp90 are lethal to yeast growth (Obermann et al., 1998; Panaretou et al., 1998) is supported by the involvement of these residues in binding of ADP. The F349A mutation of yeast Hsp90 reduced the ATPase activity by about 500-fold (Meyer et al., 2003). The corresponding residue Phe305 in HtpG is located nearby the ADP binding site, but is too distant to be directly involved in ATP hydrolysis (Figures 1B and 3A). Thus, the impact of the F349A mutation on ATP hydrolysis may be indirect, possibly via a conformational change in the active site. On the other hand, the structural data show certain inconsistencies with the mutagenesis data. The mutations R380A and Q384A of yeast Hsp90 (corresponding to R336 and Q340 of HtpG, Figure 1C) significantly lower ATPase activity and change the cell growth phenotype (Meyer et al., 2003). On basis of these mutation data and the alignment with the structure of GyrB, a catalytic loop with residues 375–388 of yeast Hsp90, in which Asn377, Arg380, and Gln384 (Asn333, Arg336, and Gln340 of HtpG) would provide γ-phosphate interactions, was proposed for ATP hydrolysis of Hsp90 (Meyer et al., 2003). This loop corresponds to residues 329–344 in HtpG and contributes to formation of helix H7 (Figures 1A and 1C). In the HtpG559-ADP-Mg structure, Arg336 orients its side chain toward ADP, but Asn333 and Gln340 swing away from the ADP site. The closest distance from an atom of this loop (NH2 of Arg336) to the model ATP is about 13 Å. Therefore, the HtpG structure would predict no direct interactions of Arg336 with ATP, although it is possible that ATP induces conformational changes to bring Arg336 to interact with the γ-phosphate of ATP. On the other hand, exposure of residues Asn333, Arg336, and Gln340 to molecular surface and their neighborhood to the ADP site may predict their roles in interaction with client proteins, thus explaining the suppression of yeast growth by their mutation.

Partially Buried Model of ATP Binding

How ATP binds and facilitates Hsp90 chaperone function has been a puzzle. Although ATP functions differently from ADP, such as bringing the N-terminal domains in contact (Prodromou and Pearl, 2003), the binding of ATP is essentially the same as ADP in yeast Hsp90 and GRP94 except for the disorder of the γ-phosphate (Prodromou et al., 1997a; Immormino et al., 2004). To understand the mechanism of Hsp90 function, we modeled ATP into the binding pocket of HtpG on the basis of superposition of the N-terminal domain of HtpG over ADPNP bound GyrB. The orientation of the γ-phosphate of ATP can be modeled in at least two ways (Figure 3C). The first orientation of the γ-phosphate of ATP is the simulation of ADPNP binding in GyrB. In this model, the γ-phosphate interacts with Lys99, a residue conserved from bacterial to human Hsp90s except for the mitochondrial TRAP1. Lys99 in the N-terminal domain of HtpG is spatially close to Lys337 of the middle domain of GyrB and may thus play a similar role as Lys337 that has been proposed to orient the γ-phosphate of ATP for a nucleophilic attack by water (Brino et al., 2000). In addition, Glu34 of HtpG, which corresponds to Glu33 of yeast Hsp90, Glu47 of human Hsp90α (Figure 1C), Glu42 of GyrB, and Glu29 of MutL, may activate a water molecule for the nucleophilic attack, as proposed earlier (Obermann et al., 1998; Prodromou et al., 1997a; Panaretou et al., 1998; Brino et al., 2000; Ban et al., 1999). Alternatively, the γ-phosphate of ATP may orient to the open space toward the middle domain. In this model, the γ-phosphate of ATP is stabilized by Lys294 that is well conserved in yeast and human Hsp90s (Figure 1C).

In the above models, the solvent-accessible area of ATP accounts for only 25% and 31%, implying that ATP is deeply buried in the pocket (Figure 1B). Thus, our structure would predict no direct contacts of ATP with residues in the neighboring monomer of Hsp90 dimer. Rather, ATP may promote conformational changes such as N-terminal domain dimerization, to facilitate the functions of Hsp90, as reviewed earlier (Meyer et al., 2003).

Conformational Changes upon ADP Binding

The binding of ADP to HtpG induces conformation changes within the monomer. The superposition of the unliganded HtpG over the ADP bound form yields rms deviations of 3.4 and 2.6 Å for the Cα atoms of residues 1–483 of chains A and 15–483 of chain B, respectively. These deviations are two to three times the differences between two monomers of each dimer of the unliganded or ADP bound HtpG (1.2 and 1.0 Å). Further superposition using the comparable residues as identified by the distance difference matrix analysis (Richards and Kundrot, 1988) yields rms deviations of 1.9, 0.7, 0.5, and 1.0 Å for the whole chain (residues 27–92 and 130–483), the N-terminal, M1, and M2 domains of chain A, and 1.2, 0.9, 0.5, and 0.7 Å for those of chain B. Thus, these numbers suggest that conformation changes mainly occur in the N-terminal domain (Figure 4A). The N-terminal β strand B1 (residues 4–8) and helix H1 (residues 12–23) of chain A show average displacements of 2.2 and 3.7 Å for their Cα atoms, which are about three and five times the rms displacement for the N-terminal domain. Although the N-terminal residues 1–26 do not directly interact with ADP, their positional shifts appear to be the consequence of ADP binding. Besides, the conformational changes and the posi-

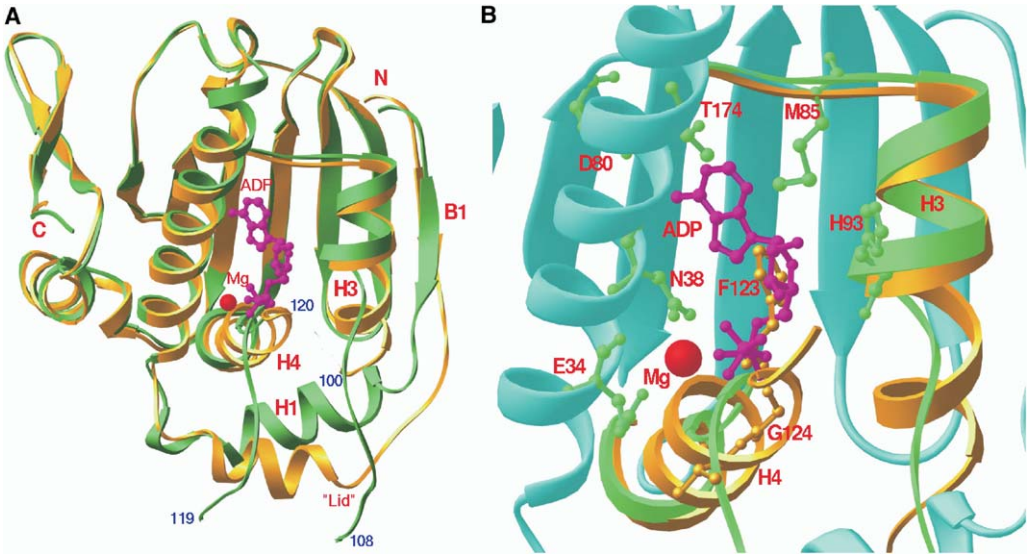

Figure 4. ADP Induces Conformation Changes

(A) The superposition of the N-terminal domain of the unliganded HtpG (golden ribbons) over HtpG-ADP-Mg (green ribbons). The N-terminal residues 1–26 (B1 and H1), the lid fragment (residues 96–125), and helices H3 and H4 undergo large positional movement or conformational change upon ADP binding. The beginning and end positions of the missing loops are marked with blue numbers.

(B) The detailed view on conformational changes around the ADP binding site. The golden and green ribbons represent the loops of the unliganded and ADP bound HtpG. The cyan ribbons represent the fragment without significant conformation changes. Unfolding of the end of H3 and the top of H4 can be seen. Phe123 and Gly124 of the unliganded HtpG would collide with the phosphate of ADP and move 7 and 13 Å for their Cα atoms, respectively.

tional movements of the lid fragment (residues 93–129) also are apparently the results of ADP binding for its direct interactions with ADP. While many residues of the lid fragment are disordered or without secondary structure elements, helices H3 (residues 87–99) and H4 (residues 122–132) have unique conformation and show significant conformation changes and positional movements (Figure 4B). The Cα atoms of the first portion of H3 (residues 92–96) show an average 1.8 Å displacement upon ADP binding, which is 2.6 times the rms deviation for the N-terminal domain. The last helical turn of H3 (residues 97–100) in the unliganded HtpG is unfolded and shows displacements of 6–14 Å for the Cα atoms (Figures 4A and 4B). Residues 121–124 of helix H4 in the unliganded HtpG collide with the phosphate group of ADP so as to convert from a helical conformation to a random coil and to migrate 7–17 Å of their Cα atoms away from ADP (Figure 4B).

Our results are consistent with the dramatic conformational changes and positional shifts of the helices 1-4-5 in the recently reported structures of GRP94 upon binding of AMP, ADP, or ATP (Immormino et al., 2004). The conformational changes of H1 (residues 12–23) upon ADP binding in HtpG are comparable with the changes of H1 in GRP94 (residues 78–92, Figure 1C). Helix H4 of GRP94 (residues 171–184) corresponds to residues 103–116 in HtpG. Unfortunately, most residues of this loop in HtpG are disordered and thus no comparison can be performed, although the dramatic change of H3 residues (97–100) in HtpG would predict significant movements of this loop. Residues 188–193 of helix H5 in GRP94 showed a large positional migration, in comparison with the helix to coil conversion of residues 121–124 in HtpG. Furthermore, clash of Gly196 in GRP94 with the phosphates (Immormino et al., 2004) is also consistent with the HtpG structures where the corresponding Gly124 collided with ADP and moved 7 Å away. Thus, the flexibility of the "lid" fragment must be an important property for the function of Hsp90. This assumption is further emphasized by the observation that the distally related member of the ATPase superfamily, the DNA mismatch protein MutL, converts the first portion of the lid fragment from a disordered conformation to a helix upon nucleotide binding (Ban et al., 1999).

Different Domain Assembly of the ATPase Superfamily Members Implies Different Mechanisms

Hsp90 is a member of the ATPase superfamily that includes ATP-dependent DNA topoisomerase II/gyrase B (GyrB), DNA repair protein MutL, and histidine kinases CheA and EnvZ (Dutta and Inouye, 2000). It has been reported that the conformation of ADP and its interactions are highly similar among these ATPase proteins (Prodromou et al., 1997a; Brino et al., 2000; Ban et al., 1999; Bilwes et al., 1999). The structural comparison with program DALI (Holm and Sander, 1993) shows various degrees of similarities between the individual domains of HtpG (residues 1–388), GyrB (residues 1–392), MutL (residues 1–331), and CheA (residues 357–539). The superposition of the N-terminal domain of HtpG (residues 1–231) over the ATPase proteins yielded rms deviations of 3.2 Å for 151 comparable residues of GyrB (Protein Data Bank entry code 1AJ6), 3.2 Å for 139 residues of MutL (1B63), and 2.7 Å for 86 residues of chemotaxis protein CheA (1B3Q). For the M1 domain of HtpG (residues 232–388), DALI comparison showed rms deviations of 3.2 Å for 94 comparable residues of

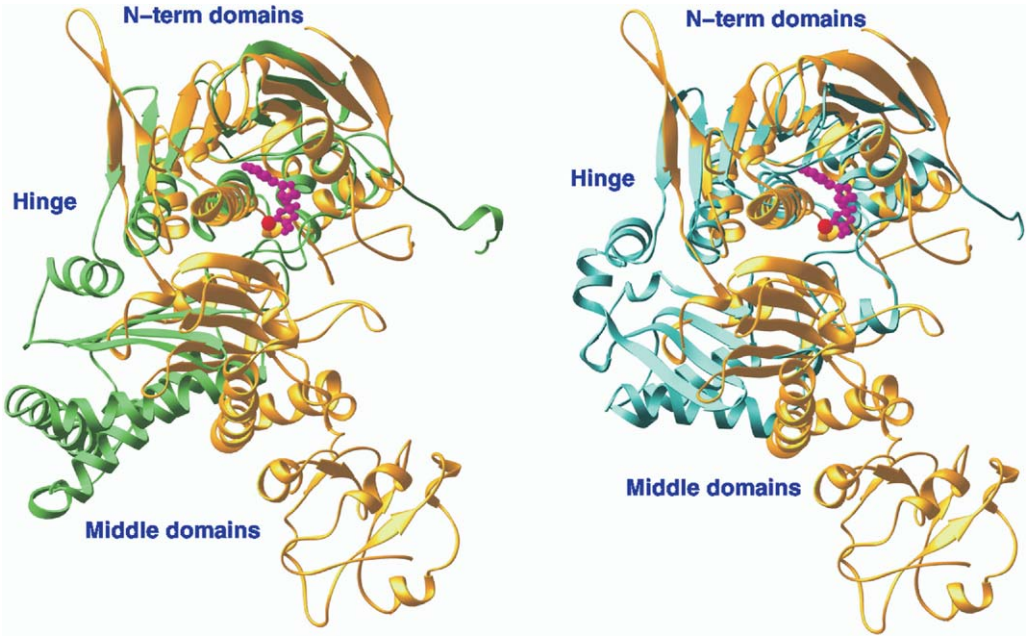

Figure 5. Superposition of HtpG over GyrB and MutL

HtpG is shown as yellow ribbons, GyrB as green ribbons (A), and MutL as cyan ribbons (B). ADP is shown as pink balls and Mg as red ball. The N-terminal and M1 domains of HtpG share similar topological folding with GyrB and MutL.

MutL (1B63) and 3.3 Å for 80 residues of yeast DNA topoisomerase II (GyrB analog, 1PVG). Graphic display of the superposition revealed that the topological folding of the individual N-terminal and M1 domains of HtpG is similar to that of GyrB and MutL, suggesting an evolutionary link among them.

However, HtpG shows substantial differences in the secondary, tertiary, and quaternary structures from other members of the ATPase superfamily. The most dramatic difference is the assembly of the N-terminal and middle domains of HtpG, GyrB, and MutL. When the N-terminal domains of the ATPase proteins are superimposed, the hinge around residue 233 of HtpG switches the middle domain of HtpG to a completely different direction from those of GyrB and MutL (Figure 5). As a consequence of the different domain assembly, the dimer structures are completely different between HtpG and GyrB/MutL.

Although illustration of the substrate binding awaits structures of the proteins in complex with their substrates, the binding pockets are predicted to be different for the members of ATPase family because of their different substrates: DNAs for GyrB and MutL, but proteins for Hsp90. This argument is rational because the different quaternary and dimer structures will make different molecular shapes and pockets for binding of substrates, and is also supported by the minor but significant variations on the conserved ATP binding. For example, Lys99 of the N-terminal domain of HtpG corresponds to middle domain Lys337 of GyrB and Lys307 of MutL, which have been proposed to fix the orientation of the γ-phosphate of ATP (Brino et al., 2000, Ban et al., 1999). Based on these observations, we speculate that the mechanisms for the biological functions of the ATPase superfamily proteins are somewhat different although they all depend on ATP activation.

Implications for the Mechanism of Hsp90 Function

The mechanism by which Hsp90 chaperones a variety of structurally distinct client proteins remains a mystery due to lack of structures of full-length Hsp90 in complex with client proteins. The best working model is the "molecular clamp" in which two monomers of Hsp90 dimerize in parallel via the C-terminal domain in a resting state and ATP drives the N-terminal dimerization to clamp a client protein binding to the middle domain (Richter and Buchner, 2001; Young et al., 2001; Prodromou and Pearl, 2003). This model is supported by biochemical studies showing that the Hsp90 fragment without the C-terminal domain is a monomer in solution but becomes a dimer in the presence of ATP (Wearsch and Nicchitta, 1996; Chadli et al., 2000; Prodromou et al., 2000; Richter et al., 2001). However, electron microscope imaging revealed two morphologies of Hsp90: a linear Hsp90 dimer in the unliganded and ADP bound states and an O-ring structure upon ATP binding or heat treatment (Maruya et al., 1999). The antibody against N-terminal region of Hsp90 modified two poles of the linear dimer and the C-terminal region antibody bound to the side of the dimer (Maruya et al., 1999), suggesting an antiparallel dimer.

The HtpG fragment 1–559 dimerizes in an antiparallel pattern in the crystal states of both unliganded and ADP bound forms, apparently in contrast to the "molecular clamp" model, but consistent with the electron microscopic and immunological studies. The gel filtration of HtpG559 in the presence or absence of ADP and ATP showed a major peak with a molecular weight of a dimer (Figure S2), implying that the dimerization scheme in the crystals may simulate the solution state. However, it remains unknown if the truncated HtpG recapitulates the dimerization of the full-length Hsp90. Nevertheless, the mutual interactions between helices H1

Table 1. Statistics of Diffraction Data and Structure Refinement

	Wavelength (Å)	Unit Cell (a, b, c [Å])	Resolution (Å)	Number of Reflections				
				Total	Unique	R_{merge}[a]	I/σ	Completeness (%)
MAD data of Se-HtpG559-ADP-Mg in space group $P2_12_12$								
Peak	0.9791	72.5, 84.2, 212.9	2.9	212,997	29,771	0.073 (0.234)	14.7 (3.0)	100 (100)[b]
Inflect	0.9792	72.5, 84.2, 212.7	3.1	158,083	22,981	0.072 (0.256)	11.7 (3.3)	93.7 (56.9)
Remote	0.9400	72.5, 84.2, 212.9	3.3	120,667	18,079	0.081 (0.285)	10.8 (2.5)	86.2 (31.2)
Native unliganded HtpG in space group $P42_12$	1.0	158.0, 158.0, 117.0	2.9	187,726	32,234	0.099 (0.429)	14.9 (2.1)	97.1 (87.1)[c]

Refinement	Unliganded HtpG	Se-HtpG559-ADP-Mg
Resolution (Å)	2.9	2.9
Reflections	30717	52300
Completeness	0.919	0.937
R factor/free	0.240/0.295	0.269/0.314
Rms deviation		
Bond (Å)	0.0088	0.094
Angle	1.5°	1.6°
Number of atoms (residues)		
Chain A	3839 (1–102, 120–489)	3866 (1–108, 117–483)
Chain B	3710 (15–98, 120–489)	3866 (1–108, 117–483)
Average B factor (Å^2)		
Chain A	67.6	61.5
Chain B	50.0	70.0
ADP		30.2
Mg		27.5

[a] Numbers in parentheses represent the statistics for the highest resolution shell.
[b] 1198 reflections at 2.9–2.8 Å resolution shell were treated as reflections at 2.9 Å resolution.
[c] 835 reflections at 2.9–2.8 Å resolution shell were treated as reflections at 2.9 Å resolution.

(residues 12–23) of the N-terminal domains of the unliganded HtpG dimer are consistent with the mutagenesis data that the mutations of E7C, Q9C, and E11C enable N-terminal dimerization of yeast Hsp90 (Prodromou et al., 2000).

In short, highly changeable interfacial regions identified in the HtpG structures may reflect conformational flexibility of Hsp90 and may be an essential character for Hsp90 to accomplish its chaperoning activities on a variety of structurally distinct client proteins. The multiple interfacial interactions in the HtpG structures may be important elements for ATP-driven dimerization, environmentally induced oligomerization, or binding of client proteins and cochaperones.

Experimental Procedures

Cloning and Purification of HtpG

The HtpG gene encoding the full-length protein (total 624 amino acids and molecular weight of 71 kDa) was cloned into plasmid pBJ935. The HtpG fragment for amino acids 1–559 (HtpG559) was subcloned from plasmid pBJ935-HtpG. A pair of oligonucleotide primers was synthesized for amplification of the HtpG coding region by PCR: T7 polymerase primer for 5′ end and primer CGG GCTTTGTTACTAGTCGGATCTTTACTAATCG containing an XhoI restriction site for 3′ end. The amplified HtpG559 cDNA and the expression vector pET3E were separately digested by the restriction enzymes NcoI and XhoI, purified from agarose gel, and then ligated by T4 DNA ligase.

The plasmids pBJ935-HtpG and pET-HtpG559 were transformed into *E. coli* BL21 (Codonplus) and grown in LB medium with appropriate antibiotics at 37°C to A600 = 0.7. The overexpression was induced by addition of 0.1 mM isopropyl β-D-thiogalactopyranoside (IPTG) at 30°C for 6 hr. Full-length HtpG and HtpG559 were purified by passing through chromatographic columns of DEAE Sepharose CL-6B (Phamacia), hydroxylapatite Bio-Gel HTP (Bio-Rad), Q-Sepharose (Phamacia), and Superdex 200 (Phamacia). A typical purification yielded 50–100 mg of full-length HtpG and HtpG559 from 1 L culture with estimated purity >95%, as judged on SDS gel. The isoelectric focusing gel showed mainly a single band at ~pH 4.2 for HtpG559.

Crystallization of Unliganded HtpG

The unliganded HtpG was crystallized by the microdialysis method against a buffer of 1.75 M ammonium sulfate, 0.1 M MES (pH 6.5), 3% DMSO, and 1 mM NaN_3. The crystals were formed in about a month and have the space group $P42_12$ with cell dimensions of a = b = 158.0 and c = 117.0 Å. The crystallographic asymmetric unit contains two molecules of HtpG. The diffraction data were collected to 2.9 Å resolution on beamline X25 of Brookhaven National Lab and processed by program HKL (Otwinowski and Minor, 1997) (Table 1).

Preparation, Crystallization, and Data Collection of Selenomethionyl HtpG559

E. coli BL21 cells carrying the pET-HtpG559 plasmid were grown in 50 ml of LB medium at 37°C overnight. The cells were centrifuged and inoculated into 1 liter of M9 minimal medium containing 0.4% glucose, 50–100 mg/liter of lysine, selenomethionine, threonine, phenylalanine, leucine, isoleucine, and valine. After growing to

A600 = 0.7, IPTG was added to induce overexpression of selenomethionyl HtpG559 (SeHtpG559) at 30°C for 6 hr. SeHtpG559 was purified using the similar method for native HtpG559. A typical purification from 1 L culture yields 50–100 mg SeHtpG559 with estimated purity >95%, as judged by SDS gel.

The SeHtpG559-ADP-Mg complex was prepared by mixing 0.4 mM SeHtpG559 with 5 mM ADP and 10 mM Mg and crystallized in two crystal forms. The first crystal form was grown by vapor diffusion against the well buffer of 17% PEG3350, 0.1 M Na acetate, 0.1 M HEPES (pH 7.5), and 5% ethylene glycol, and has the space group I222 with one molecule of SeHtpG559-ADP-Mg in the crystallographic asymmetric unit. The multiwavelength anomalous diffraction (MAD) data of SeHtpG559-ADP-Mg at three wavelengths were collected to 2.5 Å resolution on beamline X12C at Brookhaven National Lab and processed by program HKL (Otwinowski and Minor, 1997). The second crystal form of the SeHtpG559-ADP-Mg complex was crystallized by vapor diffusion against the well buffer 16% PEG3350, 0.1 M HEPES (pH 7.5), 10% glycerol. The crystals have the space group $P2_12_12$ and two molecules of SeHtpG559-ADP-Mg in the crystallographic asymmetric unit. The MAD data of SeHtpG-ADP-Mg in $P2_12_12$ at three wavelengths were collected on beamline X25 at Brookhaven National Lab (Table 1).

Structure Determination of HtpG559

The structure of HtpG559-ADP-Mg was initially determined by MAD (Hendrickson and Ogata, 1997), using the Se MAD data in the space group I222. The program SOLVE (Terwilliger and Berendzen, 1999) automatically located 10 Se sites out of 12 and yielded figure of merit of 0.45 at 2.5 Å resolution. The phases from SOLVE were improved by solvent flattening and phase combination, as implemented in the density modification package of CCP4. The ($2F_o - F_c$) map at 2.5 Å resolution showed clear electron density for the N-terminal and M1 domains (residues 1–400) in the I222 crystal system, but the trace for the residues in the M2 domain was ambiguous. Models of the HtpG559 structures were built by program O (Jones et al., 1991) and refined by program CNS (Brünger et al., 1998). The refinement on the partial structure with residues 1–400 yielded an R free of about 0.4 at 2.5 Å resolution. A careful examination showed that the I222 crystal has a pseudotranslation at about the body-center position and is not a true space group. Thus, another MAD data set in the space group $P2_12_12$ was collected. The $P2_12_12$ crystal contains two molecules in the asymmetric unit. The anomalous difference Fourier that was calculated by using the SeHtpG559 data at peak wavelength and the phases from the partial structure yielded 22 sites of Se in the space group $P2_12_12$. The refinement of the Se sites by SOLVE produced a figure of merit of 0.38 for 23935 reflections at 2.9 Å resolution. The phases were improved by solvent flattening, local symmetry-averaging, and phase combination. The electron density maps calculated from the improved MAD phases clearly showed the trace of residues 1–483. The statistics of the refinement are shown in Table 1.

The structure of unliganded HtpG was solved by the molecular replacement method using a monomer of HtpG559 as the starting model. The translation search on the first molecule yielded a correlation coefficient of 0.21 and an R factor of 0.53 for 11127 reflections between 4 to 8 Å resolution. The correlation coefficient and R factor were improved to 0.25 and 0.52 when the second molecule is included. The model was built against an averaged map and refined by CNS (Table 1).

Supplemental Data

Supplemental data are available online at http://www.structure.org/cgi/content/full/13/4/579/DC1/.

Acknowledgments

We thank beamlines X25 and X12C at Brookhaven National Laboratory for the data collection. This research is supported by National Institutes of Health grants GM059791 to H.K. and DK46249 to D.T.

Received: September 20, 2004
Revised: December 7, 2004
Accepted: December 10, 2004
Published: April 11, 2005

References

Ali, J.A., Jackson, A.P., Howells, A.J., and Maxwell, A. (1993). The 43-kilodalton N-terminal fragment of the DNA gyrase B protein hydrolyzes ATP and binds coumarin drugs. Biochemistry *32*, 2717–2724.

Ban, C., Junop, M., and Yang, W. (1999). Transformation of MutL by ATP binding and hydrolysis: a switch in DNA mismatch repair. Cell *97*, 85–97.

Bilwes, A., Alex, L.A., Crane, B.R., and Simon, M.I. (1999). Structure of CheA, a signal-transducing histidine kinase. Cell *96*, 131–141.

Blagosklonny, M.V. (2002). Hsp-90-associated oncoproteins: multiple targets of geldanamycin and its analogs. Leukemia *16*, 455–462.

Brino, L., Urzhumtsev, A., Mousli, M., Bronner, C., Mitschler, A., Oudet, P., and Moras, D. (2000). Dimerization of Escherichia coli DNA-gyrase B provides a structural mechanism for activating the ATPase catalytic center. J. Biol. Chem. *275*, 9468–9475.

Brünger, A.T., Adams, P.D., Clore, G.M., DeLano, W.L., Gros, P., Grosse-Kunstleve, R.W., Jiang, J.S., Kuszewski, J., Nilges, M., Pannu, N.S., et al. (1998). Crystallography & NMR system: a new software suite for macromolecular structure determination. Acta Crystallogr. D Biol. Crystallogr. *54*, 905–921.

Buchner, J. (1999). Hsp90 & Co.—a holding for folding. Trends Biochem. Sci. *24*, 136–141.

Caplan, A.J. (1999). Hsp90's secret unfold: new insights from structural and functional studies. Trends Cell Biol. *9*, 262–268.

Carsons, M. (1991). Ribbons 2.0. J. Appl. Crystallogr. *24*, 958–961.

Chadli, A., Bouhouche, I., Sullivan, W., Stensgard, B., McMahon, N., Catelli, M.G., and Toft, D.O. (2000). Dimerization and N-terminal domain proximity underlie the function of the molecular chaperone heat shock protein 90. Proc. Natl. Acad. Sci. USA *97*, 12524–12529.

Csermely, P., and Kahn, C.R. (1991). The 90 kDa heat-shock protein (Hsp90) possesses an ATP binding site and autophosphorylation activity. J. Biol. Chem. *266*, 4943–4950.

Csermely, P., Schnaider, T., Soti, C., Prohaszka, Z., and Nardai, G. (1998). The 90-kDa molecular chaperone family: structure, function and clinical application, a comprehensive review. Pharmacol. Ther. *79*, 129–168.

Dutta, R., and Inouye, M. (2000). GHKL, an emergent ATPase/kinase superfamily. Trends Biochem. Sci. *25*, 24–28.

Ferrarini, M., Heltai, S., Zocchi, M.R., and Rugarli, C. (1992). Unusual expression and localization of heat-shock proteins in human tumor cells. Int. J. Cancer *51*, 613–619.

Goetz, M.P., Toft, D.O., Ames, M.M., and Erlichman, C. (2003). The Hsp90 chaperone complex as a novel target for cancer therapy. Ann. Oncol. *14*, 1169–1176.

Harris, S.F., Shiau, A.K., and Agard, D.A. (2004). The crystal structure of the carboxy-terminal dimerization domain of htpG, the Escherichoa coli Hsp90, reveals a potential substrate binding site. Structure *12*, 1087–1097.

Hendrickson, W.A., and Ogata, C.M. (1997). Phase determination from multiwavelength anomalous diffraction measurements. Methods Enzymol. *276*, 494–523.

Holm, L., and Sander, C. (1993). Protein structure comparison by alignment of distance matrices. J. Mol. Biol *233*, 123–138.

Hunter, T., and Poon, R.Y.C. (1997). Cdc37: a protein kinase chaperone? Trends Cell Biol. *7*, 157–161.

Immormino, R.M., Dollins, D.E., Shaffer, P.L., Soldano, K.L., Walker, M.A., and Gewirth, D.T. (2004). Ligand-induced conformational shift in the N-terminal domain of GRP94, an Hsp90 chaperone. J. Biol. Chem. *279*, 46162–46171.

Isaacs, J.S., Xu, W., and Neckers, L. (2003). Heat shock protein

90 as a molecular target for cancer therapeutics. Cancer Cell *3*, 213–217.

Jez, J.M., Chen, J.C., Rastelli, G., Stroud, R.M., and Santi, D.V. (2003). Crystal structure and molecular modeling of 17-Dmag in complex with human Hsp90. J. Chem. Biol. *10*, 361–368.

Jones, T.A., Zou, J.-Y., Cowan, S.W., and Kjeldgaard, M. (1991). Improved methods for building protein models in electron density maps and the location of errors in these models. Acta Crystallogr. A *47*, 110–119.

MacLean, M., and Picard, D. (2003). Cdc37 goes beyond Hsp90 and kinases. Cell Stress Chaperones *8*, 114–119.

Maruya, M., Sameshima, M., Nemoto, T., and Yahara, I. (1999). Monomer arrangement in Hsp90 dimer as determined by decoration with N and C-terminal region specific antibodies. J. Mol. Biol. *285*, 902–907.

Mayer, M.P., and Bukau, B. (1999). Molecular chaperones: the busy life hsp90. Curr. Biol. *9*, R322–R325.

Meyer, P., Prodromou, C., Hu, B., Vaughan, C., Roe, S.M., Panaretou, B., Piper, P., and Pearl, L.H. (2003). Structural and functional analysis of the middle segment of Hsp90: implications for ATP hydrolysis and client protein and cochaperone interactions. Mol. Cell *11*, 647–656.

Meyer, P., Prodromou, C., Liao, C., Hu, B., Roe, S.M., Vaughan, C.K., Vlasic, I., Panaretou, B., Piper, P.W., and Pearl, L.H. (2004). Structural basis for recruitment of the ATPase activator Aha1 to the Hsp90 chaperone machinery. EMBO J *23*, 511–519.

Nadeau, K., Sullivan, M.A., Bradley, M., Engman, D.M., and Walsh, C.T. (1992). 83-kilodalton heat-shock proteins of trypanasomes are potent peptide-stimulated ATPases. Prot. Sci. *1*, 970–979.

Nadeau, K., Das, A., and Walsh, C.T. (1993). Hsp90 chaperonins possess ATPase activity and bind heat chock transcription factors and peptidyl prolyl isomerases. J. Biol. Chem. *268*, 1479–1487.

Neckers, L. (2002). Hsp90 inhibitors as novel cancer chemotherapeutic agents. Trends Mol. Med. *8*, S55–S61.

Nemoto, T., Sato, N., Iwanari, H., Yamashita, H., and Takagi, T. (1997). Domain structures and immunogenic regions of the 90-kDa heat-shock protein (Hsp90). Probing with a library of anti-Hsp90 monoclonal antibodies and limited proteolysis. J. Biol. Chem. *272*, 26179–26187.

Nicholls, A., Sharp, K.A., and Honig, B. (1991). Protein folding and association: insights from the interfacial and thermodynamic properties of hydrocarbons.. Prot. Struct. Funct. Genet. *11*, 281–296.

Obermann, W.M.J., Sondermann, H., Russo, A., Pavletich, N.P., and Hartl, F.U. (1998). In vivo function of Hsp90 is dependent on ATP binding and ATP hydrolysis. J. Cell Biol. *143*, 901–910.

Otwinowski, Z., and Minor, W. (1997). Processing of X-ray diffraction data collected in oscillation mode. Methods Enzymol. *276*, 307–326.

Owen, B.A., Sullivan, W.P., Felts, S.J., and Toft, D.O. (2002). Regulation of heat shock protein 90 ATPase activity by sequences in the carboxyl terminus. J. Biol. Chem. *277*, 7086–7091.

Panaretou, B., Prodromou, C., Roe, S.M., O'Brien, R., Ladbury, J.E., Piper, P.W., and Pearl, L.H. (1998). ATP binding and hydrolysis are essential to the function of the Hsp90 molecular chaperone in vivo. EMBO J. *17*, 4829–4836.

Pearl, L.H., and Prodromou, C. (2000). Structure and in vivo function of Hsp90. Curr. Opin. Struct. Biol. *10*, 46–51.

Picard, D. (2002). Heat-shock protein *90*, a chaperone for folding and regulation. Cell. Mol. Life Sci. *59*, 1640–1648.

Pratt, W.B. (1997). The role of the Hsp90-based chaperone system in signal transduction by nuclear receptors and receptors signaling via map kinase. Annu. Rev. Pharmacol. Toxicol. *37*, 297–326.

Pratt, W.B., and Toft, D.O. (1997). Steroid receptor interactions with heat shock protein and immunophilin chaperones. Endocr. Rev. *18*, 306–360.

Pratt, W.B., and Toft, D.O. (2003). Regulation of signaling protein function and trafficking by the Hsp90/hsp70-based chaperone machinery. Exp. Biol. Med. *228*, 111–133.

Pratt, W.B., Galigniana, M.D., Harrell, J.M., and DeFranco, D.B. (2004). Role of Hsp90 and the Hsp90-binding immunophilins in signaling protein movement. Cell. Signal. *16*, 857–872.

Prodromou, C., and Pearl, L.H. (2003). Structure and functional relationships of Hsp90. Curr. Cancer Drug Targets *3*, 301–323.

Prodromou, C., Roe, S.M., O'Brien, R., Ladbury, J.E., Piper, P.W., and Pearl, L.H. (1997a). Identification and structural characterization of the ATP/ADP-binding site in the Hsp90 molecular chaperone. Cell *90*, 65–75.

Prodromou, C., Roe, S.M., Piper, P.W., and Pearl, L.H. (1997b). A molecular clamp in the crystal structure of the N-terminal domain of the yeast Hsp90 chaperone. Nat. Struct. Biol. *4*, 477–482.

Prodromou, C., Panaretou, B., Chohan, S., Siligardi, G., O'Brien, R., Ladbury, J.E., Roe, S.M., Piper, P.W., and Pearl, L.H. (2000). The ATPase cycle of Hsp90 drives a molecular 'clamp' via transient dimerization of the N-terminal domains. EMBO J. *19*, 4383–4392.

Richards, F.M., and Kundrot, C.E. (1988). Identification of structural motifs from protein coordinate data: secondary structure and first-level supersecondary structure. Proteins *3*, 71–84.

Richter, K., and Buchner, J. (2001). Hsp90: chaperoning signal transduction. J. Cell. Physiol. *188*, 281–290.

Richter, K., Muschler, P., Hainzl, O., and Buchner, J. (2001). Coordinated ATP hydrolysis by the Hsp90 dimer. J. Biol. Chem. *276*, 33689–33696.

Richter, K., Reinsteins, J., and Buchner, J. (2002). N-terminal residues regulate the catalytic efficiency of the Hsp90 ATPase cycle. J. Biol. Chem. *47*, 44905–44910.

Roe, S.M., Prodromou, C., O'Brien, R., Ladbury, J.E., Piper, P.W., and Pearl, L.H. (1999). Structural basis for inhibition of the Hsp90 molecular chaperone by the antitumor antibiotics radicicol and geldanamycin. J. Med. Chem. *42*, 260–266.

Roe, S.M., Ali, M.M., Meyer, P., Vaughan, C.K., Panaretou, B., Piper, P.W., Prodromou, C., and Pearl, L.H. (2004). The mechanism of Hsp90 regulation by the protein kinase-specific cochaperone p50(cdc37). Cell *116*, 87–98.

Scheibel, T., Weikel, T., and Buchner, J. (1998). Two chaperone sites in Hsp90 differing in substrate specificity and ATP dependence. Proc. Natl. Acad. Sci. USA *95*, 1495–1499.

Siligardi, G., Panaretou, B., Meyer, P., Singh, S., Woolfson, D.N., Piper, P.W., Pearl, L.H., and Prodromou, C. (2002). Regulation of Hsp90 ATPase activity by the co-chaperone Cdc37p/p50cdc37. J. Biol. Chem. *277*, 20151–20159.

Soldano, K.L., Jivan, A., Nicchitta, C.V., and Gewirth, D.T. (2003). Structure of the N-terminal domain of GRP94. Basis for ligand specificity and regulation. J. Biol. Chem. *278*, 48330–48338.

Smith, D.F., and Toft, D.O. (1993). Steroid receptors and their associated proteins. Mol. Endocrinol. *7*, 4–11.

Stebbins, C.E., Russo, A.A., Schneider, C., Rosen, N., Hartl, F.U., and Pavletich, N.P. (1997). Crystal structure of an Hsp90-geldanamycin complex: targeting of a protein chaperone by an antitumor agent. Cell *89*, 239–250.

Terwilliger, T.C., and Berendzen, J. (1999). Automated structure solution for MIR and MAD. Acta Crystallogr. D Biol. Crystallogr. *55*, 849–861.

Wearsch, P.A., and Nicchitta, C.V. (1996). Endoplasmic reticulum chaperone GRP94 subunit assembly is regulated through a defined oligerization domain. Biochemistry *35*, 16760–16769.

Weikl, T., Muschler, P., Richter, K., Veit, T., Reinstein, J., and Buchner, J. (2000). C-terminal regions of Hsp90 are important for trapping the nucleotide during the ATPase cycle. J. Mol. Biol. *303*, 583–592.

Welch, W.J., and Feramisco, J.R. (1982). Purification of the major mammalian heat shock proteins. J. Biol. Chem. *257*, 14949–14959.

Whitesell, L., Sutphin, P.D., Pulcini, E.J., Martinez, J.D., and Cook, P.H. (1998). The physical association of multiple molecular chaperone proteins with mutant p53 is altered by geldanamycin, an Hsp90-binding agent. Mol. Cell. Biol. *18*, 1517–1524.

Wigley, D.B., Davies, G.J., Dodson, E.J., Maxwell, A., and Dodson,

G. (1991). Crystal structure of an N-terminal fragment of the DNA gyrase B protein. Nature *351*, 624–629.

Young, J.C., Schneider, C., and Hartl, F.U. (1997). In vitro evidence that Hsp90 contains two independent chaperone sites. FEBS Lett. *418*, 139–143.

Young, J.C., Moarefi, I., and Hartl, F.U. (2001). Hsp90: a specialized but essential protein-folding tool. J. Cell Biol. *154*, 267–273.

Yufu, Y., Nishimura, J., and Nawata, H. (1992). High constitutive expression of heat shock protein 90 alpha in human acute leukemia cells. Leuk. Res. *16*, 597–605.

Accession Numbers

The coordinates and structure factors have been deposited into the Protein Data Bank with accession codes of 1Y4S and 1Y4U.